Journal of Inflammation Research Dovepress

Open Access Full Text Article ORIGINAL RESEARCH

Unveiling the Molecular Links Between Atrial Fibrillation and Atherosclerosis: Insights into Shared Pathogenesis and Ferroptosis Diagnostic Biomarkers

Bowen Xu[1,2,*], Hongye Li[1,2,*], Hongping Chen[3], Da Teng[1,2], Lei Gong[2], Lin Zhong[2], Jun Yang[2]

[1]Qingdao Medical College of Qingdao University, Qingdao, Shandong, 266000, People's Republic of China; [2]Department of Cardiology, Yantai Yuhuangding Hospital, Yantai, Shandong, 264000, People's Republic of China; [3]Department of Cardiology, The Affiliated Hospital of Xuzhou Medical University, Xuzhou, Jiangsu, 221000, People's Republic of China

*These authors contributed equally to this work

Correspondence: Lin Zhong; Jun Yang, Email linzhongyhd1971@sina.com; yangjyhd@hotmail.com

Objective: Atherosclerosis(AS) is a vascular disease characterized by the development of plaque in the arteries, and atrial fibrillation (AF) is a common heart arrhythmia. These two conditions share several risk factors in common, such as aging, diabetes, obesity, and hypertension. Ferroptosis is a new mode of non-apoptotic cell death that plays a key role in cardiomyocyte death and has been associated with a variety of cardiac diseases. This study aimed to investigate the ferroptosis biomarkers and underlying biological mechanisms associated with AF and AS.

Materials and Methods: The gene expression dataset was obtained from GEO database, differentially expressed genes (DEGs) and ferroptosis expressed genes (FDGs) were obtained by data processing and screening, and then functional enrichment, network construction, transcription factor prediction, identification of biomarkers by LASSO and SVM - RFE algorithms, and also immune infiltration analyses and cellular experiments were performed.

Results: In AF and AS, 1627 and 571 DEGs were identified respectively, and 128 were intersected, and 47 common FDGs were also identified. Gene Ontology (GO) and Kyoto Encyclopedia of Genes and Genomes (KEGG) analysis of DEGs revealed that they were associated with biological processes and pathways such as leukocyte immunity, and FDGs were also involved in specific functions and pathways. Fifteen key genes were identified, CSF1R and ITGAM expression differences were verified, and seven transcription factors were predicted to be differentially expressed. Characterized genes were screened to construct models with good diagnostic efficacy, and immune infiltration showed that NUPR1 was associated with altered immune environments, and WB indicated that NUPR1 was highly expressed in the disease model.

Conclusion: Our study demonstrates that the ferroptosis gene NUPR1 plays a role in the pathogenesis of atrial fibrillation and atherosclerosis, and also provides valuable insights into their molecular mechanisms, which may contribute to the development of new targets and strategies for the treatment of these diseases.

Keywords: atrial fibrillation, AF, atherosclerosis, AS, ferroptosis, CSF1R, ITGAM, NUPR1

Introduction

Atrial fibrillation (AF), the most prevalent cardiac arrhythmia, has become more widespread globally as the population ages.[1,2] Despite advances in management, a considerable risk of morbidity and death still exists. The prevention of AF and its associated complications remains a challenge, and this multifactorial arrhythmia is intertwined with common concurrent cardiovascular diseases and is a classic cardiovascular risk factor.[3–6] One such cardiovascular condition commonly associated with AF is atherosclerosis (AS). AS is characterized by arterial wall damage leading to plaque formation, vessel narrowing, and reduced blood flow.[7–9] Both AF and AS share several risk factors, including aging,

Received: 23 July 2024
Accepted: 7 November 2024
Published: 13 November 2024

obesity, diabetes, and hypertension, suggesting potential common pathophysiological mechanisms.[10–12] The pathogenesis of AS involves multiple cellular processes, including endothelial dysfunction, oxidative stress, inflammation, and vascular smooth muscle cell alterations.[8,9,13,14]

Recent research has highlighted the role of ferroptosis, a novel form of regulated cell death, in cardiovascular diseases. Unlike apoptosis, necrosis, or autophagy, ferroptosis is characterized by iron accumulation, mitochondrial changes, and lipid peroxidation.[15–17] While the mechanisms linking AF and AS are not fully understood, emerging evidence suggests that inflammatory processes and oxidative stress may represent common pathways in both conditions.[18]

The objective of this research is to find similar genetic signatures between AF and AS by thorough transcriptional profiling, potentially revealing common molecular pathways that could explain their frequent coexistence and provide new insights for both conditions.

Materials and Methods

Data Collection

We obtained gene expression datasets from GEO (http://www.ncbi.nlm.nih.gov/geo), a public database. Using the search terms atherosclerosis(AS) and atrial fibrillation (AF). Following was decided upon as the inclusion criteria: 1. The included test products should be from human beings 2. Two separate expression profiles, and comprise a high number of samples (≥30). Finally, download four microarray datasets (GSE41177, GSE2240, GSE28829, GSE100927). The GSE41177 dataset comprises 32 pairs of patients with AF and 6 pairs of patients with sinus rhythm. The GSE2240 dataset has 20 pairs of patients with AF and 40 pairs of sinus rhythm, we utilize the GPL96 platform, which has 10 pairs of patients with AF and 20 pairs of sinus rhythm, which is used for validation. The GSE28829 dataset comprises of 13 early AS Composed of sclerotic plaque samples and 16 advanced atherosclerotic plaque samples. GSE100927 comprised of 35 non-atherosclerotic plaque samples and 69 atherosclerotic plaque samples, which were utilized for validation. Data analysis and collation were done out using R software (version 4.2.3) and Perl software (v5.30.0).

Screening Differentially Expressed Genes(DEGs) in AF and AS

The expression profiles of the two sets of GEOs were transformed into gene expression matrices using Perl software, and R was used to batch-correct the data sets to get normalized expression levels. Log transformation and DEGs screening were done on the normalized data using the "Limma" and "Pheatmap" packages in R software. $|logFC| > 0.585$ and adjusted P-values <0.05 were selected as threshold thresholds of statistical significance for DEGs samples. The "VennDiagram" tool in R software was used to collect their public DEGs, and 128 genes were obtained.

Screening Ferroptosis Differentially Expressed Genes(FDGs) in AF and AS

Then we downloaded the latest Ferroptosis-related genes from the website (http://www.zhounan.org/ferrdb/current/), and analyzed the difference of iron death-related genes in GSE41177 and GSE28829 datasets.172 Ferroptosis differential genes (FDGs) were obtained in the AF group and 109 in the AS group. Taking the intersection of the two finally obtained 47 FDGs.

Enrichment Analysis of DEGs

The Gene Ontology (GO) and Kyoto Encyclopedia of Genes and Genomes (KEGG) enrichment analysis of these 128 genes was done using the "clusterProfiler" package in R. The GO enrichment analysis split the gene biological function into three parts: cellular component (CC), molecular function (MF), and biological process (BP); KEGG is a database connected to important metabolic and signal transduction pathways. Where p-values and adjusted p-values are both < 0.05.

Protein-Protein Interaction (PPI) Network Construction and Hub Gene Analysis

Use the Search Tool for the Retrieval of Interacting Genes/Proteins (STRING, https://string-db.org/) to identify PPIs in DEGs. STRING is a database that looks for connections between proteins, including direct or indirect interactions. Interactions with a cumulative score of higher than 0.4 were judged statistically significant, and 0.7 was eventually picked. Use Cytoscape (version 3.9.1) to visualize this PPI network. The essential functional modules were examined utilizing Cytoscape plug-in molecular complex identification technology (MCODE). Set the selection criteria to be: node density cutoff = 0.1, node score cutoff = 0.2, K-core = 2, max depth = 100, and ultimately get 4 sub-networks. Obtain the hub genes using the CytoHubba plug-in in Cytoscape program.

GeneMANIA Network Construction and Functional Enrichment

GeneMANIA (http://www.genemania.org/), which is frequently used to generate hypotheses about gene function, evaluate gene lists, and choose genes for functional inquiry, created a co-expression network comprising these hub genes. The involved module hub genes were then subjected to GO and KEGG analyses using R software.

Verification of Hub Genes Expression

Expression of the identified hub gene was validated in GSE2240 and GSE100927. The data of the two groups were compared using *t*-test, and the P value was < 0.05.

Prediction of Transcription Factors (TFs) and Validation

Transcriptional Regulatory Relationships Unraveled by Sentence-based Text mining (TRRUST, https://www.grnpedia.org/trrust/) is a regulatory network used to predict transcription factors(TFs) and the regulatory link between the target gene of transcription factors and transcription factors. Eight hundred human TFs and eighty-two mouse TFs are connected to 6552 and 8444 regulatory targets, respectively, in the current version of TRRUST. The TRRUST database provided the TFs for the regulatory hub genes, with P value < 0.05. We utilize these TFs in GSE41177 and GSE28829 to determine if there are differences.

Identification of AS and AF Ferroptosis Gene Biomarkers

The glmnet package was used to use the least absolute shrinkage and selection operator (LASSO) method to minimize the dimensionality of the data. The FDGs between AS and AF patients and normal samples were kept for feature selection, and LASSO algorithms were used to find the gene biomarkers for AS and AF. The average misjudgement rates of their 10-fold cross-validations were used to compare the support vector machine-recursive feature elimination (SVM-RFE) model, which was created with an SVM. Additionally, overlapping biomarkers produced from the two algorithms were used to find the best gene biomarkers for AS and AF. By computing the receiver operating characteristic (ROC) curve and calculating the area under the curve (AUC), accuracy, sensitivity, and specificity, the best gene biomarkers' diagnostic potential was evaluated.

Immunoinfiltration Analysis

CIBERSORT, an algorithm for analyzing the gene expression profile to determine the cell composition of complex tissues. In this work, we used the GSE41177 and GSE28829 datasets from CIBESORT to estimate the proportion of 22 kinds of invading immune cell types in each tissue. The total analyzed immune cell type fractions for each sample were equal to 1.

Cell Culture

The American Typical Culture Collection (Manassas, VA, USA) is where HL-1 and THP-1 were obtained. AF modeling: HL-1 cells were cultured in DMEM/F12 medium (Sparkjade, China) containing 10% fetal bovine serum (FBS) (BI, Israel), and 1% penicillin-streptomycin (MCE, USA) at 37 °C with 5% CO2. As previously reported in investigations,[19,20] HL-1 cells were tachypaced using a YC-3 stimulator (Nanjing, China). The cells were stimulated

at 10 hz using 1.5 V/cm pulse voltage and square pulses lasting 5 ms. AS modeling: As we have done before, THP-1 cells were utilized to promote differentiation into the AS model.[21] The cells were cultivated at 37 °C with 5% CO2 in 1640 medium (BI, Israel), which included 10% fetal bovine serum (FBS) (BI, Israel), 5% β-mercaptoethanol (Sigma, USA), and 1% penicillin-streptomycin (MCE, USA). To create atherosclerotic macrophages for more research, phorbol 12-myristate-13-acetate (PMA) (Sigma, USA) was treated for 24 hours, and then oxidized-LDL (80 μg/mL) (Yiyuan Bio, China) was added for 48 hours.

Western Blot Analysis

Proteins were extracted from treated cells, The total protein concentrations in cells were measured using the BCA Kit. Western blotting was performed according to standard protocols. The following targets were incubated on membranes: NUPR1 (YT8077, Immunoway, China); and GAPDH (D110016, BBI, China). The ECL substrate chemiluminescence solution (E422-01, Vazyme China) was applied uniformly to the membranes. The gray value of each band was quantified using the ImageJ software.

Result

Identification of Differentially Expressed Genes in AF and AS

The GSE41177 dataset comprises 32 pairs of patients with AF and 6 pairs of patients with sinus rhythm. The GSE28829 dataset comprises 13 samples of early AS plaques and 16 samples of late atherosclerotic plaques. The expression files of GEO were evaluated using $|\log2\ FC| > 0.585$ and corrected p-value < 0.05, with batch correction. The former tested a total of 1627 DEGs, comprising 780 up-regulated genes and 847 down-regulated genes, whereas the latter screened a total of 571 DEGs, including 161 up-regulated genes and 410 down-regulated genes. The heat map displayed the 50 most significantly up- and down-regulated genes, and the differentially expressed genes were then taken as an intersection and represented as a Venn diagram (Figure 1A and B), of which 104 were co-up-regulated genes and 24 were co-down-regulated genes. These visualizations were done using heat maps and volcano maps (supplementary Figure 1).

Identification FDGs in AF and AS

The 172 and 109 FDGs identified from the GSE41177 and GSE28829 datasets, respectively, were differentially expressed compared to normal samples. Clustered heatmaps showed the expression patterns of FDGs in the samples (supplementary Figure 2). The intersection of these two groups of FDGs was later taken and 47 common genes were obtained (supplementary Figure 2). The correlation between these genes in is shown in Figure 2A and B.

Functional Enrichment Analysis of DEGs

To investigate the biological processes and pathways involved, 94 frequently occurring DEGs were submitted to GO and KEGG pathway enrichment analyses. These genes were primarily enriched in leukocyte-mediated immunity, leukocyte movement, phagocytosis, processing of antigens, MHC class II presentation of peptide antigens, and positive control of cytokine production, according to the results of the GO analysis (Figure 1C–E), all $p<0.05$. In terms of KEGG pathways, Staphylococcus aureus infection, Phagosome, and Tuberculosis were three highly enriched pathways (Figure 1F and G), all p0.05. These findings imply that the emergence and progression of both illnesses are concurrently influenced by leukocyte-mediated immunity and positive control of response to external stimulation (Figure 1E).

Functional Enrichment Analysis of FDGs

GO enrichment and KEGG pathway analysis were carried out to clarify the biological processes and pathways connected to the FDGs. Therefore, GO enrichment studies revealed that the function of "cellular response to chemical and oxidative stress" was substantially connected to FDGs of AF and AS (Figure 3A-F). Lipid and atherosclerosis, autophagy, and the FoxO signaling pathway were shown to be abundant in KEGG pathway studies (Figure 3G-J). These pieces of data suggested that FDGs may be involved in the control of autophagy and oxidative stress, which may contribute to their potential role in the pathogenesis of AF and AS.

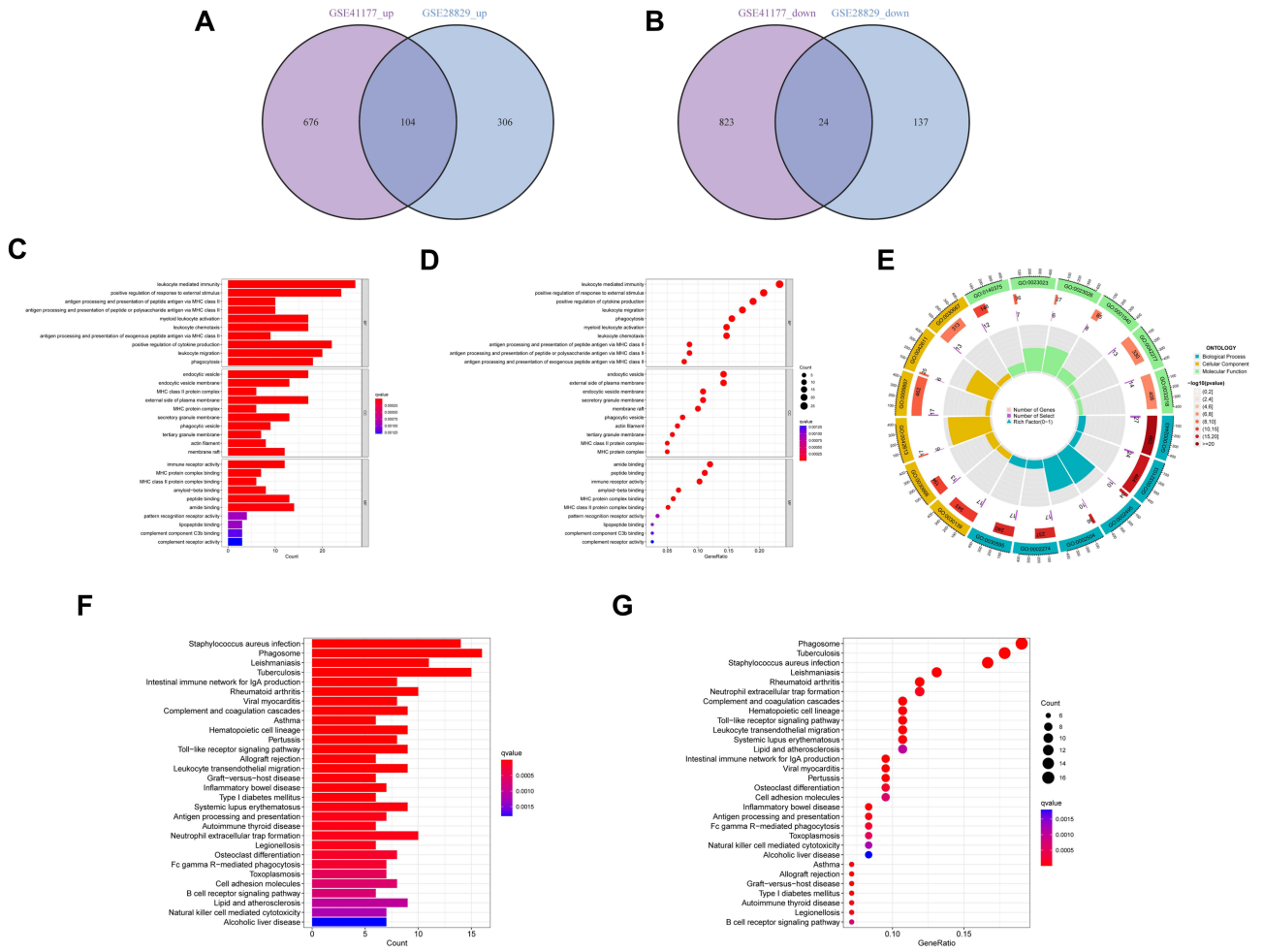

Figure 1 (**A**) These two data sets demonstrate the upregulation of 104 DEGs that overlap. (**B**) These two data sets demonstrate the downregulation of 24 overlapping DEGs.(**C**) The GO enrichment analysis histogram (**D**) Bubble plot of GO analysis. (**E**) Circle diagram showing the analysis of GO enrichment. (**F**) The KEGG pathway analysis histogram. (**G**) A KEGG pathway analysis bubble diagram. The threshold for significance was an adjusted P value <0.05.

DEGs PPI Network Construction and Selection of Hub Genes

Using Cytoscape, a PPI network with 80 nodes and 248 interaction pairings was created for frequent DEGs with a composite score higher than 0.7 (Figure 4A). The top 15 hub genes were determined by utilizing the Cytoscape plug-in's cytoHubba feature and using degree as the scoring type, including LY86, ITGAM, CSF1R, TYROBP, FCER1G, TLR2, HLA-DRA, ITGB2, CD14, LYN, C1QB, CD86, LILRB2, HCK, and VAV1 (Figure 4B and Table 1). With the help of the GeneMANIA database, we investigated the co-expression network and related functions of these genes. With 69.88% coexpression, 20.59% physical interaction, 3.98% pathway, 3.12% colocalization, and 2.44% prediction, these genes displayed a sophisticated PPI network. (Figure 4C). The MCODE component of Cytoscape was used to derive four closely related gene modules, comprising 31 shared DEGs and 63 interaction pairings (Figure 4D-G).

Functional Analysis of Hub Genes

We conducted GO and KEGG pathway enrichment analysis to examine the biological pathways and functions of hub genes. According to the results of the GO analysis, these genes were primarily involved in phagocytosis, Cellular reactions to compounds of bacterial origin and lipopolysaccharides, the effective controlling of immune effector mechanisms, cellular responses to biotic stimuli, positive regulation of leukocyte activation, leukocyte-mediated immunity, and positive regulation of response to external stimuli (Figure 5A–C). The results show that leukocyte immune responses and cellular immunological effects have an influence on both illnesses. They are implicated

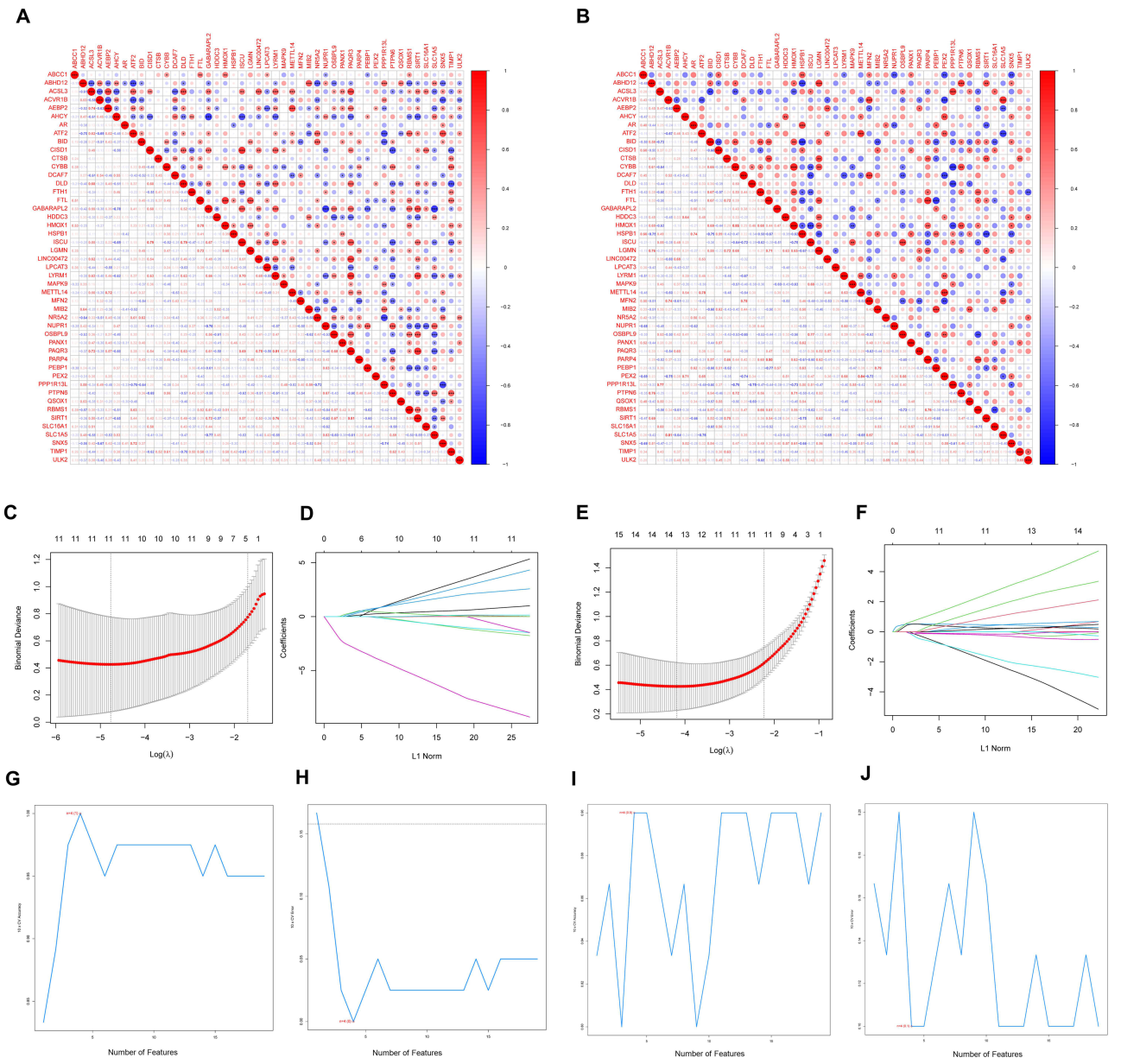

Figure 2 (**A** and **B**) The correlation of FDGs between AF and AS. (**C** and **D**) 11 AF-related characteristics were chosen using the LASSO logistic regression approach with penalty parameter adjustment carried out using 10-fold cross-validation. Similar to (**E** and **F**), 14 AS-related characteristics were obtained.(**G** and **H**) SVM-RFE algorithm to filter the 4 FDGs to find the ideal mashup of feature genes. The ideal AF feature genes were ultimately found to be 4 genes. (**I** and **J**) Four AS optimum features were also obtained. *p < 0.05; **p < 0.01; ***p < 0.001.

in Staphylococcus aureus infection, Hematopoietic cell lineage, Phagosome, Pertussis, Leishmaniasis, Tuberculosis, and Legionellosis, according to KEGG pathway analysis (Figure 5D–F). GO and KEGG enrichment data show a substantial correlation between hub genes and the immune system.

Validation of Hub Genes

To validate these hub genes' reliable expression levels. We chose two more datasets that had atherosclerotic plaques and AF, and we examined how much these hub genes were expressed in those datasets. Only CSF1R and ITGAM genes were shown to be downregulated in AF as compared to normal tissue, according to the findings (Figure 6A). In comparison to healthy vascular tissue, atherosclerotic plaques had greater expression levels of the genes CSF1R, ITGAM, TLR2, FCER1, TYROBP, and LY86 (Figure 6B).

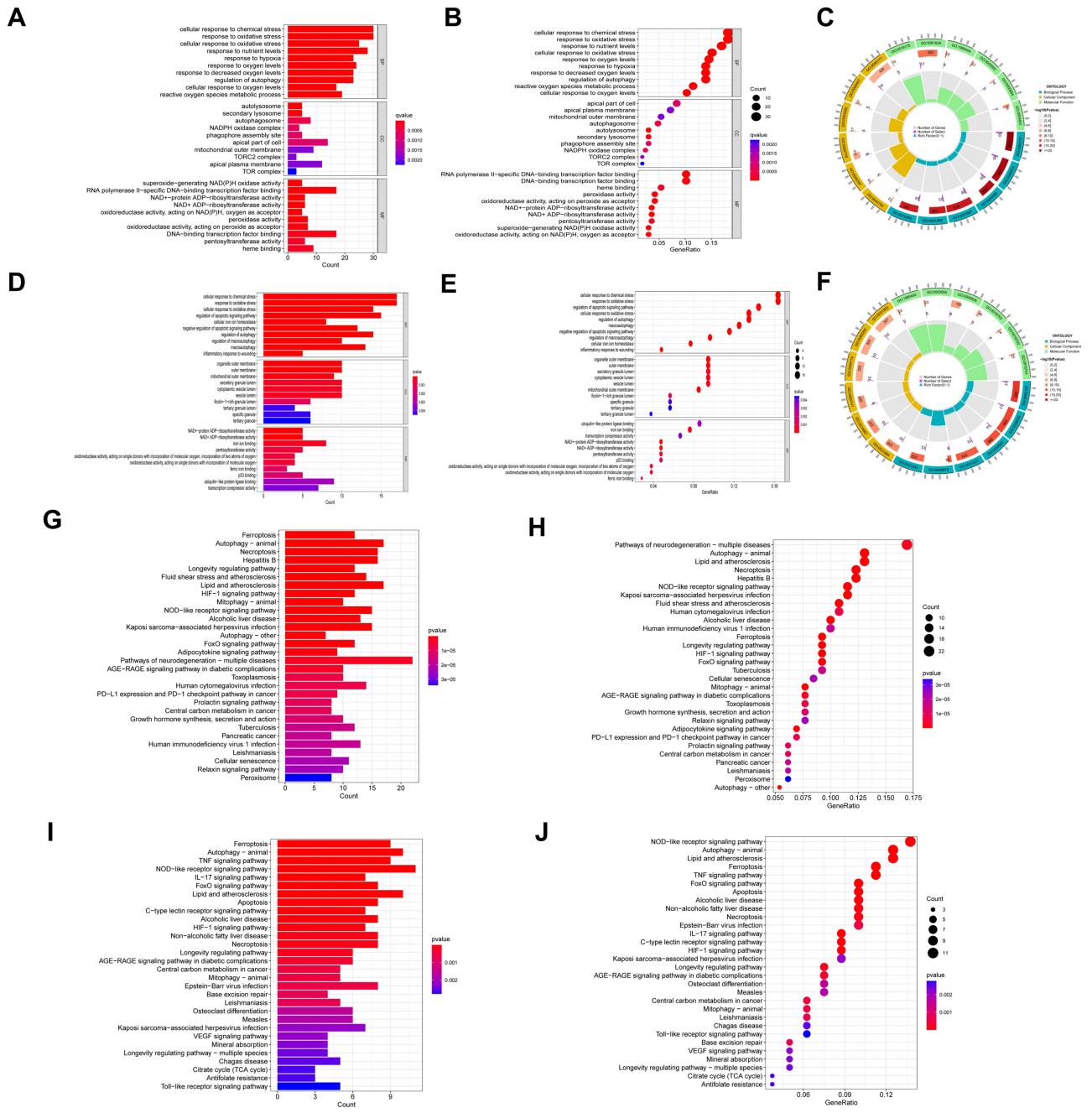

Figure 3 Functional analyses for the FDGs. (**A-F**) GO enrichment studies revealed that the function of "cellular response to chemical and oxidative stress" was substantially connected to FDGs of AF and AS. (**G-J**) KEGG pathway analyses indicate Lipid and atherosclerosis, autophagy, and the FoxO signaling pathway were enriched.

Prediction of TFs and Validation

Seven transcription factors (TFs) that may regulate the expression of these genes were found using the TRRUST database (Figure 7A and Table 2). We discovered that the transcription factors HIF1A, SPI1, and TRERF1 were substantially expressed in AF (Figure 7B) to provide additional support. While transcription factor TRERF1 was reduced in atherosclerotic plaques, transcription factors RELA and SPI1 were upregulated (Figure 7C).

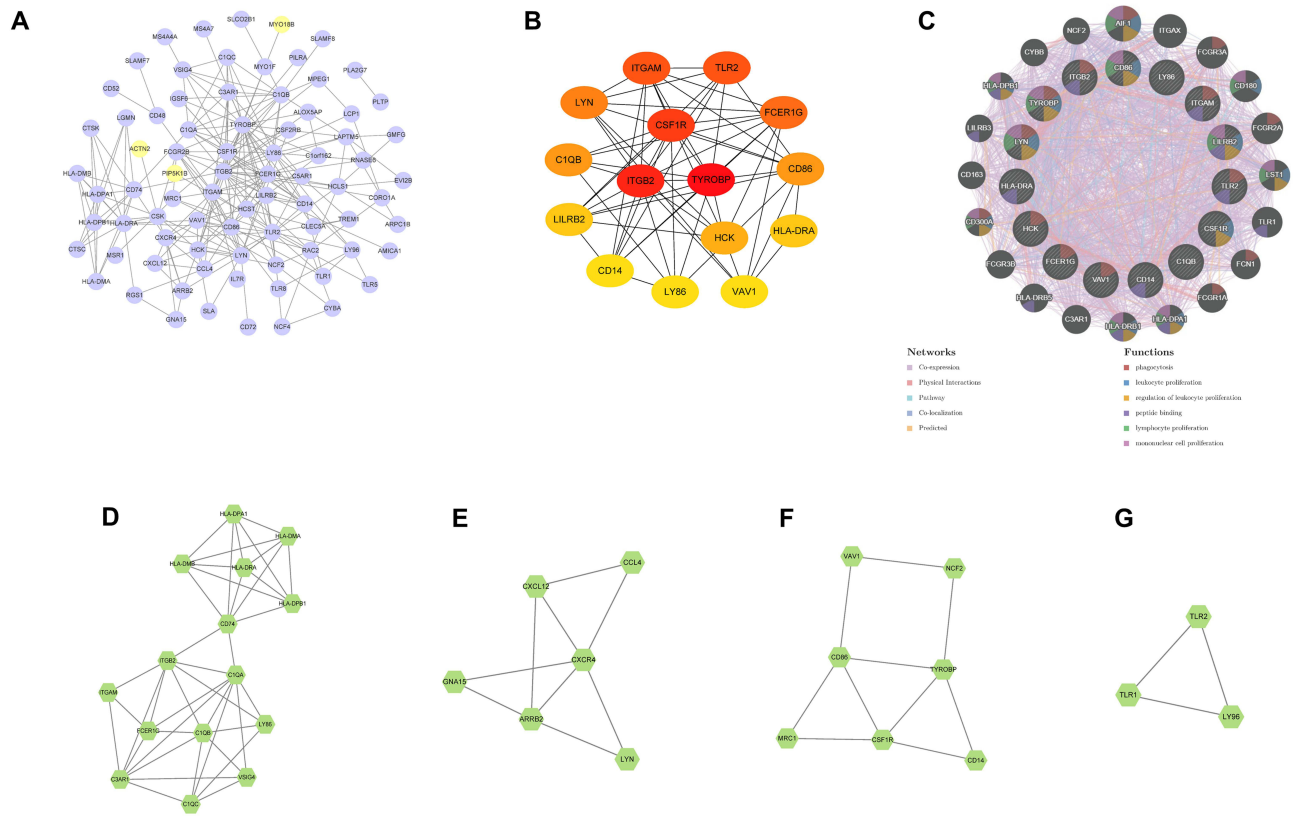

Figure 4 (**A**) PPI network diagram. Champagne yellow denotes down-regulated genes, whereas lavender blue denotes up-regulated genes. (**B**) Cytoscape was used to screen 15 overlapping hub genes; the deeper the hue, the more likely the gene is a network core gene.(**C**) GeneMANIA was used to evaluate the hub genes and the genes that co-expressed with them. Four important gene clustering modules are shown in (**D**–**G**).

2 FDGs Identified as Co-Diagnostic Genes for AS and AF

Considering the differences between AF and AS patients and healthy individuals, we aimed to estimate the diagnostic potential of FDGs (Figure 2A and B). Next, we used two different machine learning algorithms, LASSO and SVM-RFE, in the GSE41177 and GSE28829 datasets to screen for important FDGs that can differentiate between AF, AS, and normal individuals. We used the LASSO logistic regression algorithm to screen for 11 features associated with AF, adjusting the penalty parameter through 10-fold cross-validation. We used the LASSO logistic regression algorithm to filter out 11 features associated with AF (Figure 2C and D) and 14 features associated with AS (Figure 2E and F). Then, we used the SVM-RFE algorithm to screen the FDGs of AF and AS to determine the best combination of feature genes. Finally, four genes (maximum accuracy = 1, minimum RMSE = 0) were identified as the best feature genes for AF (Figure 2G and H), and the best feature genes for AS were also four (Figure 2I and J) (maximum accuracy = 0.9, minimum RMSE = 0.1). Crossover of marker genes obtained from the LASSO model of AF and the SVM-RFE model identified 2 marker genes (NOX5, ADAMTS13) for subsequent analyses (Figure 8A), and using the same approach, 4 genes (CTSB, CP, NUPR1, PARP12) were identified in the model crossover for AS. Regrettably, we did not find AF intersecting with AS in several of the characterized genes, but we used these characterized genes to intersect with the previous 47 FDGs, and we obtained two Ferroptosis-related genes, CTSB, and NUPR1, and were associated with both AF, AS. Based on the above four marker genes, we built a logistic regression model using the R package glm, and the subsequent ROC curves showed that the logistic regression model based on the four marker genes could discriminate between normal samples and AFsamples, with AUCs of at least 0.781 (Figure 8B). In addition, ROC curves for the marker genes were generated to elucidate the ability of individual genes to distinguish AF and normal samples. As shown in Figure 8C, the AUC of all genes was 1. Meanwhile, normal and AS samples had an AUC of at least 0.846 (Figure 8D)

Table 1 Top 15 hub Gene Scores

Node_name	MCC	DMNC	MNC	Degree	EPC	Bottleneck	Eccentricity	Closeness	Radiality	Betweenness	Stress	Clustering Coefficient
LY86	1	0.47886	10	1	14.869	3	0.24375	38.83333	3.6974	130.67155	660	0.43636
ITGAM	1	0.44065	15	1	17.169	7	0.325	43.83333	3.95065	800.06075	2792	0.32353
CSF1R	1	0.42605	18	1	17.831	2	0.325	43.5	3.9	317.39795	1470	0.37908
TYROBP	1	0.31982	24	1	19.556	13	0.325	48.83333	4.1026	1104.31658	3630	0.21846
FCER1G	1	0.41061	15	1	16.695	6	0.325	43	3.91266	311.46895	1596	0.34167
TLR2	1	0.27524	17	1	15.917	6	0.325	43.66667	3.93799	549.88683	1996	0.25
HLA-DRA	8	0.37893	4	4	7.425	1	0.24375	30.75	3.21623	3.13799	26	0.66667
ITGB2	6	0.64826	5	3	5.008	1	0.195	28.15	2.86169	0	0	1
CD14	201	0	1	11	3.242	1	0.195	25.58333	2.7224	0	0	0
LYN	4	0.66569	6	3	11.406	2	0.24375	34.33333	3.43149	153.15404	544	0.66667
C1QB	393	0	1	14	2.206	1	0.195	23.5	2.50714	0	0	0
CD86	135	0.30779	2	9	4.942	1	0.24375	28.83333	3.10227	0	0	1
LILRB2	4	0.28529	6	3	8.256	1	0.24375	31.66667	3.21623	23.52383	96	0.4
HCK	17	0.30779	2	5	5.747	1	0.24375	29.25	3.06429	7.81746	32	0.33333
VAV1	1	0.3063	24	1	19.389	13	0.325	49.33333	4.19123	1281.57541	4634	0.24638

https://doi.org/10.2147/JIR.S488288

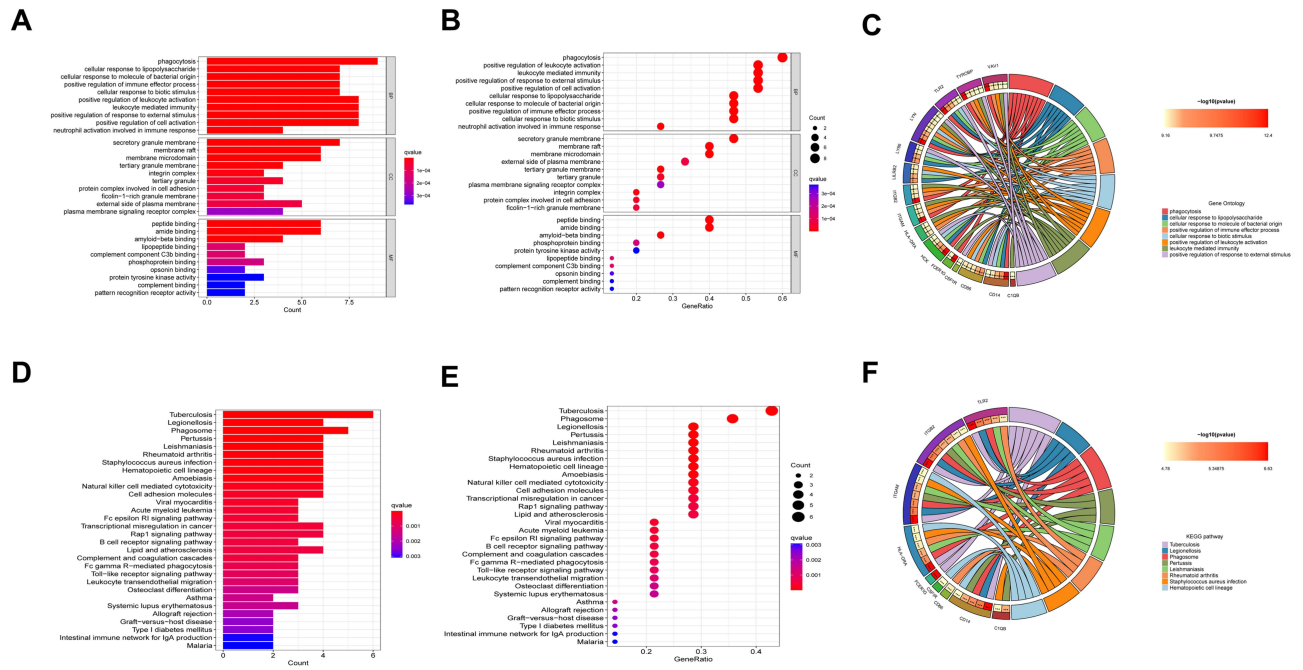

Figure 5 GO and KEGG pathway enrichment analysis. (**A-C**) Analysis of GO enrichment (**D-F**) analysis of KEGG pathway enrichment.

for the former and 1 (Figure 8E) for the latter. The above evidence suggests that the logistic regression model is more accurate and specific than individual marker genes in distinguishing AF, AS and normal samples.

CTSB and NUPR1 are Closely Related to AF, AS-Related Pathways

To further explore the potential function of marker genes to distinguish disease samples from normal samples, we performed single-gene GSEA-KEGG pathway analysis. The first 6 pathways enriched for each marker gene are shown in Figure 9. After comprehensive analysis, we found that in AF, these CTSBs were enriched in "natural killer cell-mediated cytotoxicity", "nitrogen metabolism", "PPAR signaling pathway", "starch and fructose metabolism", "steroid hormone biosynthesis", and "alanine-leucine and isoleucine degradation"; whereas, in AS, these CTSBs were enriched in "cytokine signaling pathway", cytokine- cytokine receptor interactions", this has the same result as NUPR1 enrichment in AF.

Analysis of Immune Cell Infiltration Landscape in AF, AS Patients

The earlier findings suggested that AF, AS and the immunological microenvironment are inextricably linked.[22–24] The earlier findings suggested that AF, AS and the immunological microenvironment are inextricably linked. In order to investigate the variations in the immune microenvironment between AF, AS patients and normal samples, we developed the CIBERSORT technique. According to Figure 10A and B, whereas T-cell follicular helper, Macrophages M2 were more expressed in normal samples than in AF samples, which had a larger number of plasma cells, monocytes, and neutrophils. B cells memory, macrophages M0, and macrophages M2 were more prevalent in AS samples than in normal samples, although T cells regulatory (Tregs), mast cells resting, and macrophages M0 were more prevalent in normal samples. As compared to the normal sample, AS, AF had a higher percentage of T cells gamma delta, but less dendritic cells that were activated. In addition, Pearson correlation analysis revealed that Mast cells resting and activated had strong positive and negative correlations with NUPR1 in AF. CTSB was positively correlated with macrophages M0 while NUPR1 was negatively correlated with NK cells resting in AS (Figure 10C and D). These pieces of information suggested that NUPR1 may be related to modifications in the immune milieu of AF, AS patients.

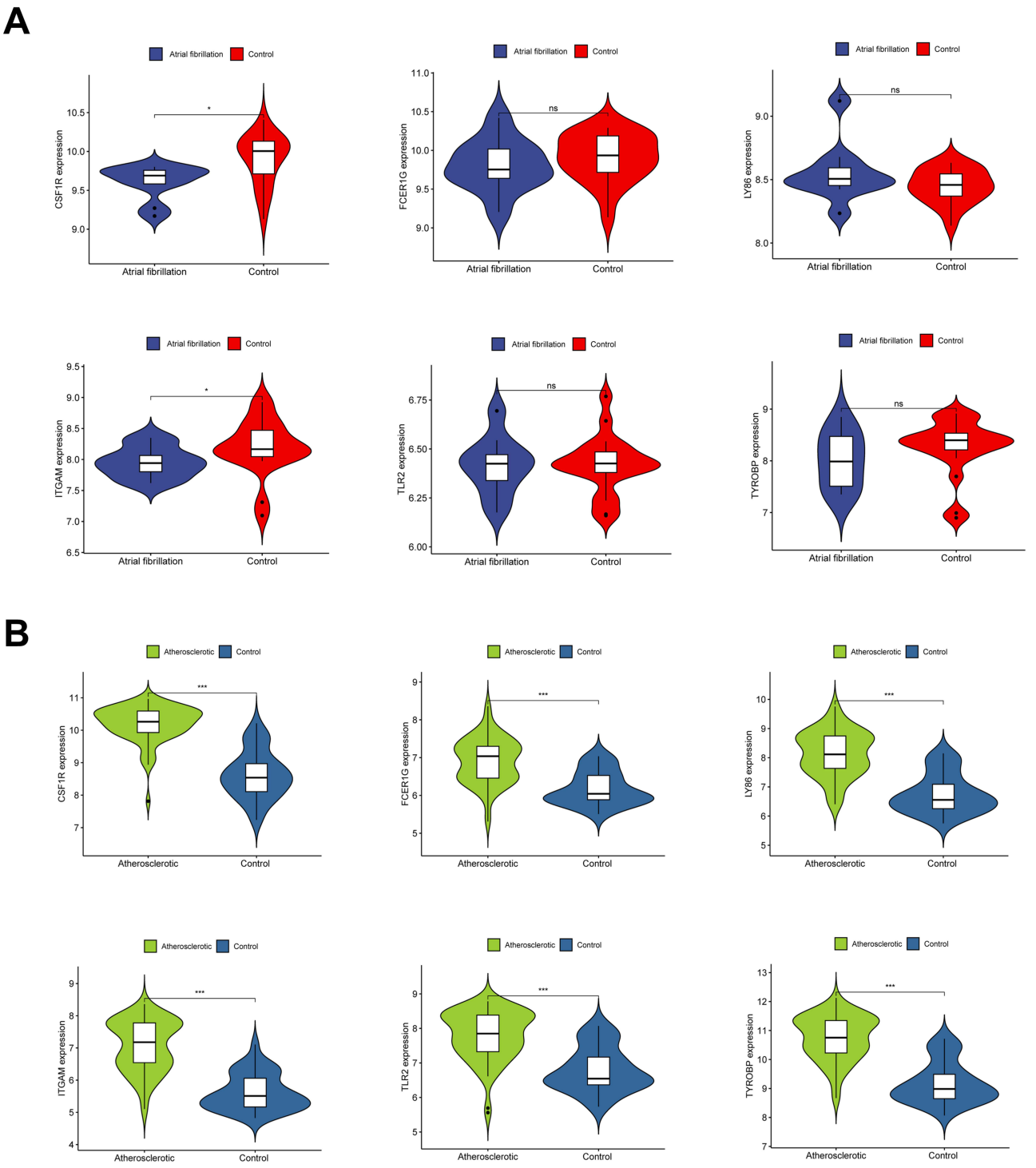

Figure 6 (**A**) The expression level of the hub gene in GSE2240. A comparison of data between the two groups was performed using the mean *t*-test. p-value <0.05 was considered statistically significant. *P<0.05; **P<0.01; ***P<0.001. (**B**) The expression level of the hub gene in GSE100927. A comparison of data between the two groups was performed using the mean *t*-test. p values < 0.05 were considered statistically significant. ns, not significant,*P<0.05; ***P<0.001.

Expression of NUPR1 in AF and AS Models

The expression of NUPR1 in AF and AS model was detected by Western blotting. The results showed that NUPR1 were weakly expressed in the normal model and strongly expressed in AF and AS models (Figure 11A-D).

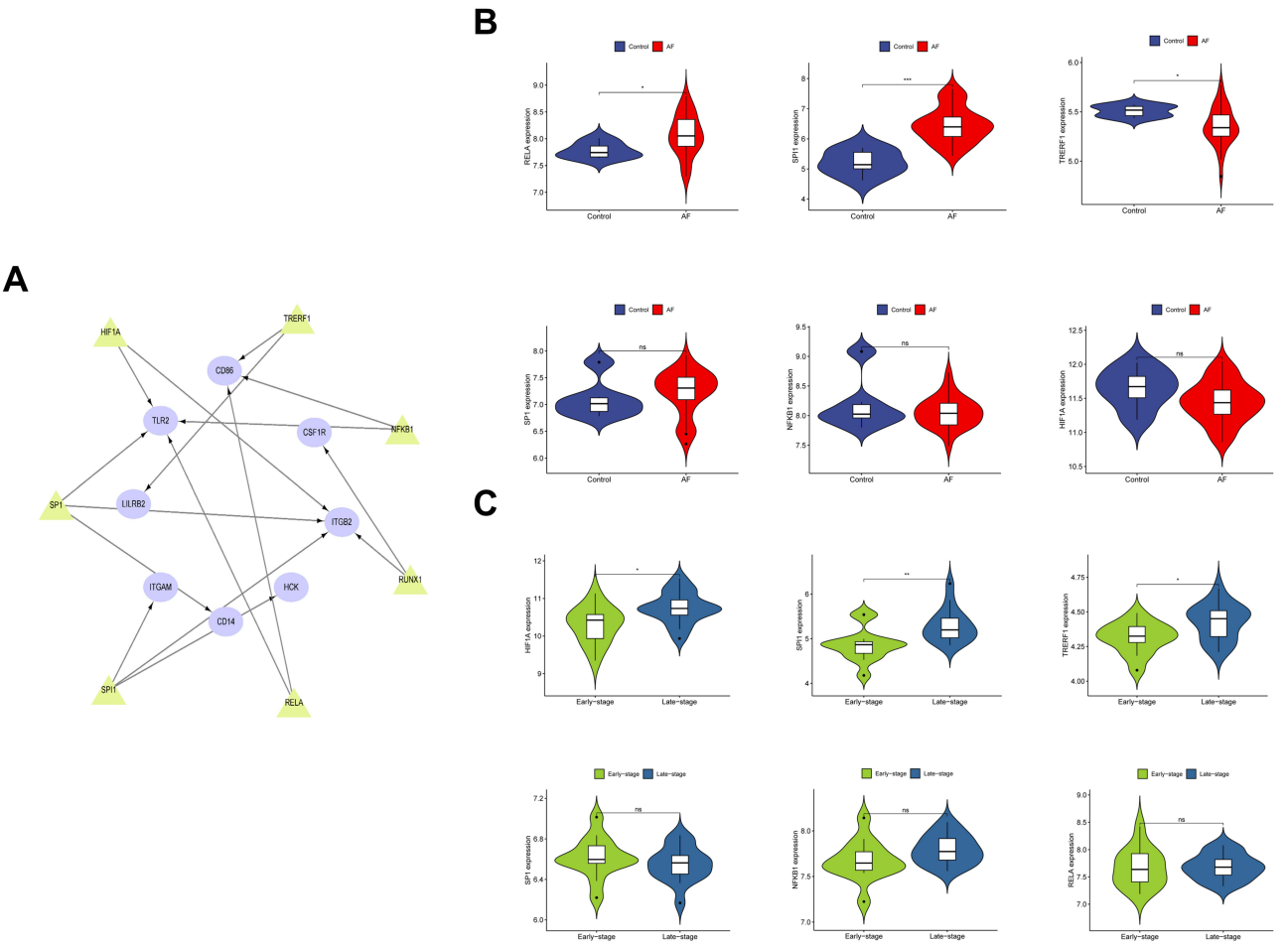

Figure 7 (**A**) TFs regulate the network. TFs are in the periphery, marked in light green, and hub genes are in the middle, marked in light purple. (**B** and **C**) Expression levels of TFs in GSE41177 and GSE28829. Comparison of data between the two groups was performed using the mean *t*-test. p values < 0.05 were considered statistically significant. ns, not significant, *p < 0.05; **p < 0.01; ***p < 0.001.

Discussion

In this study, we identified 128 shared DEGs between AF and AS conditions, along with 47 ferroptosis-related genes (FDGs) common to both diseases. Notably, CSF1R and ITGAM were identified as potential co-diagnostic markers, while NUPR1 emerged as a key ferroptosis-related gene involved in both conditions. Functional enrichment analysis revealed that these genes are mostly engaged in immune system functions, oxidative stress pathways, and inflammatory responses. The identification of FDGs represents a novel finding, suggesting that ferroptosis, an iron-dependent programmed cell death process, may serve as a crucial mechanistic link between AF and AS. Particularly, NUPR1, as a ferroptosis-related gene may be crucial in controlling the mechanisms that lead to cell death in both conditions, potentially providing novel targets for treatment.

Table 2 Key Transcriptional Factors (TFs) of Hub Genes

Key TF	Description	Of Overlapped Genes	P value	Q value	List of Overlapped Genes
TRERF1	Transcriptional regulating factor 1	2	1.24E-05	5.23E-05	CD86, LILRB2
SPI1	Spleen focus forming virus (SFFV) proviral integration oncogene spi1	3	1.49E-05	5.23E-05	ITGAM, HCK, ITGB2
RUNX1	Runt-related transcription factor 1	2	0.000452	0.00105	ITGB2, CSF1R
HIF1A	Hypoxia inducible factor 1, alpha subunit (basic helix-loop-helix transcription factor)	2	0.00193	0.00338	TLR2, ITGB2
SP1	Sp1 transcription factor	3	0.00565	0.00792	ITGB2, TLR2, CD14
RELA	v-rel reticuloendotheliosis viral oncogene homolog A (avian)	2	0.0232	0.0235	CD86, TLR2
NFKB1	Nuclear factor of kappa light polypeptide gene enhancer in B-cells 1	2	0.0235	0.0235	CD86, TLR2

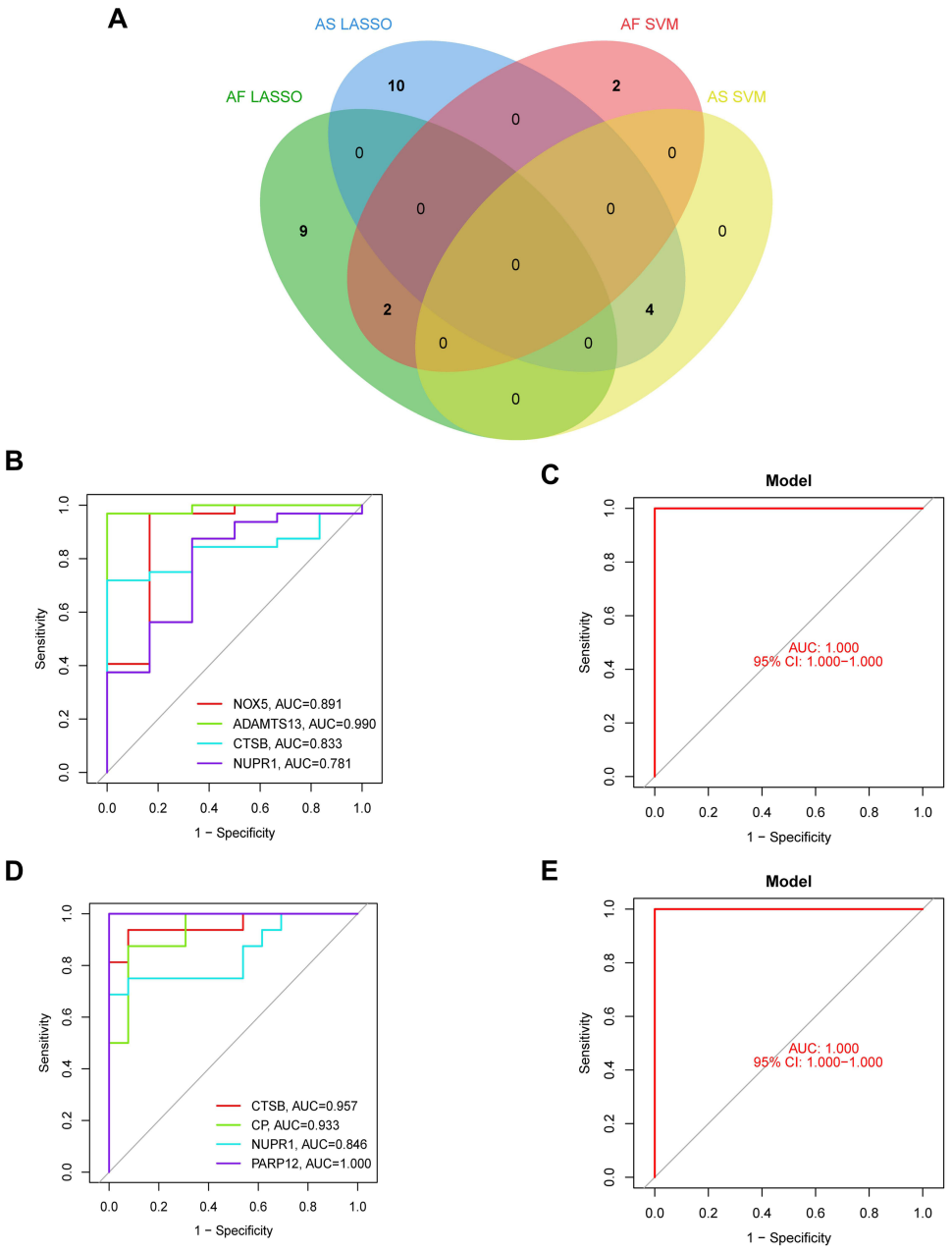

Figure 8 (**A**) The marker genes obtained from the AF, AS LASSO and SVM-RFE models. (**B** and **D**) Logistic regression model to identify the AUC of AF, AS samples. (**C** and **E**) ROC curves for the 4 marker genes of AF, AS.

Our results have important clinical practice implications. The identification of CSF1R and ITGAM as co-diagnostic markers could potentially improve early detection strategies for both AF and AS. A diagnostic panel for risk stratification might be created using these indicators and the ferroptosis-related gene NUPR1. Previous studies have primarily focused on individual disease markers, whereas our integrated approach provides a more comprehensive understanding of the shared pathogenic mechanisms. This could lead to more effective targeted therapies addressing both conditions simultaneously.

Our study provides some new insights compared to the studies by Wei et al and Wu et al[25,26] We found both overlap and new contributions. While previous studies explored the association between AF and AS, our study delves into the specific genetic mechanisms between the two and highlights the role of FDGs in both diseases. Unlike previous studies that have

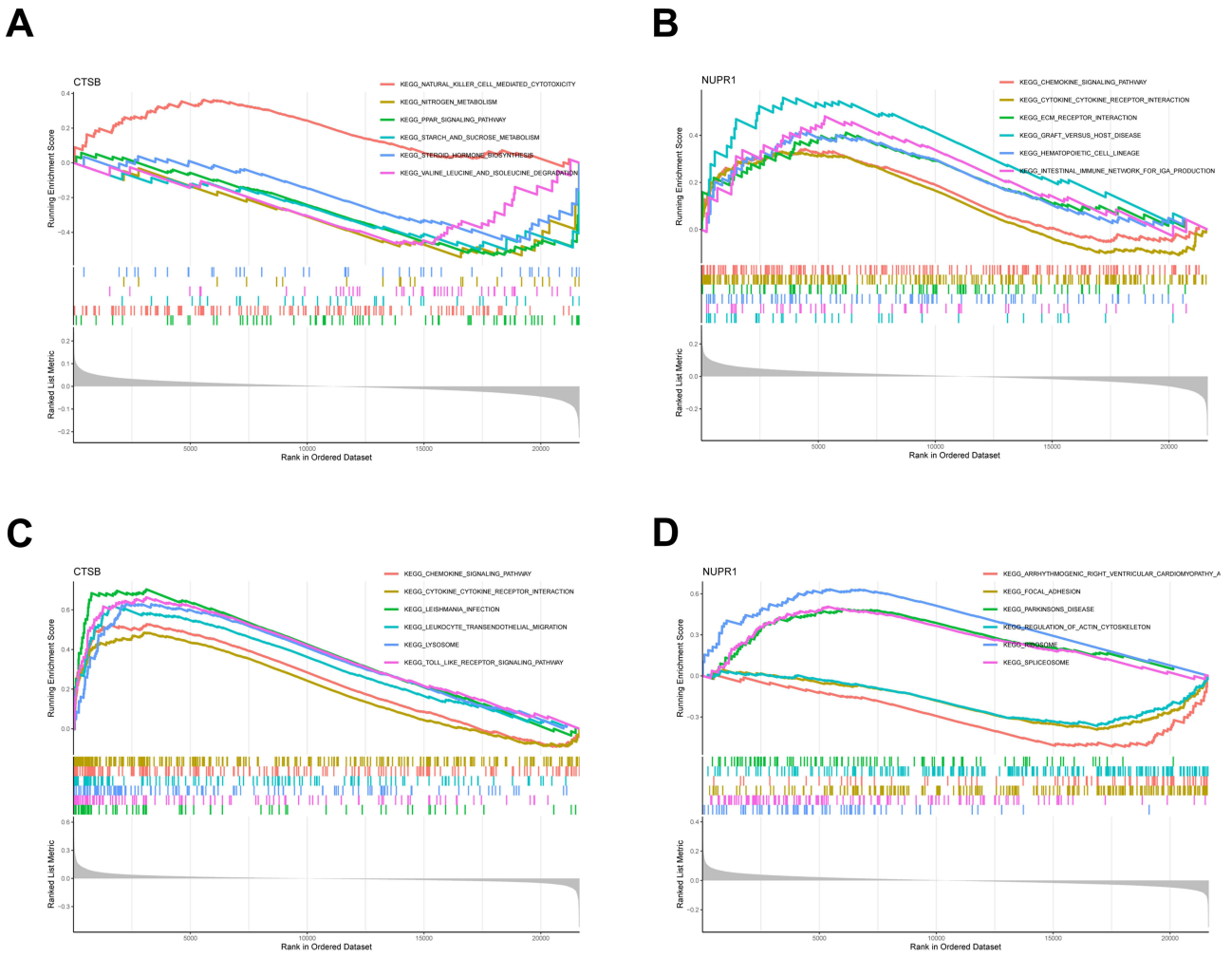

Figure 9 AF, AS Single-gene GSEA-KEGG pathway analysis in CTSB (**A** and **C**), NUPR1 (**B** and **D**).

focused primarily on clinical outcomes and risk factors, our approach emphasises the genetic basis and common pathways of AF and AS. This distinction is critical as it allows us to propose potential therapeutic targets based on gene expression profiles.

The relationship between AF and AS has been well proven in previous studies. Risk factors such as age, hypertension, diabetes, gender and obesity contribute to the development of both diseases.[1,10,11,27] The underlying mechanisms may involve inflammation, endothelial dysfunction and platelet-mediated thrombosis.[1,10–12] Local hemodynamic changes appear to be the primary mechanism in AF development. AS, stenosis, and carotid plaque formation can result from carotid endothelial injury due to abnormal blood flow.[28]

Inflammation biomarkers play a crucial role in predicting cardiovascular events in AF patients.[18,29] Studies have shown the importance of various biomarkers, including IL-6, GDF-15, CRP, and cTnI in AF patients.[30–33] Our findings regarding CSF1R and ITGAM add to this growing list of potential biomarkers, particularly highlighting their role in both AF and AS pathogenesis.

The enrichment analysis of the DEGs provided further insights into the biological functions and pathways that may be dysregulated in AF and AS. The gene ontology (GO) analysis identified cellular components, molecular functions, and biological processes associated with the DEGs.[5] KEGG analysis revealed key pathways potentially involved in disease development, particularly highlighting the role of inflammatory and immune response processes.

However, our study still has some limitations. First, our study was based on the analysis of public databases, and further validation of these results in clinical samples is needed. Second, while we performed functional enrichment

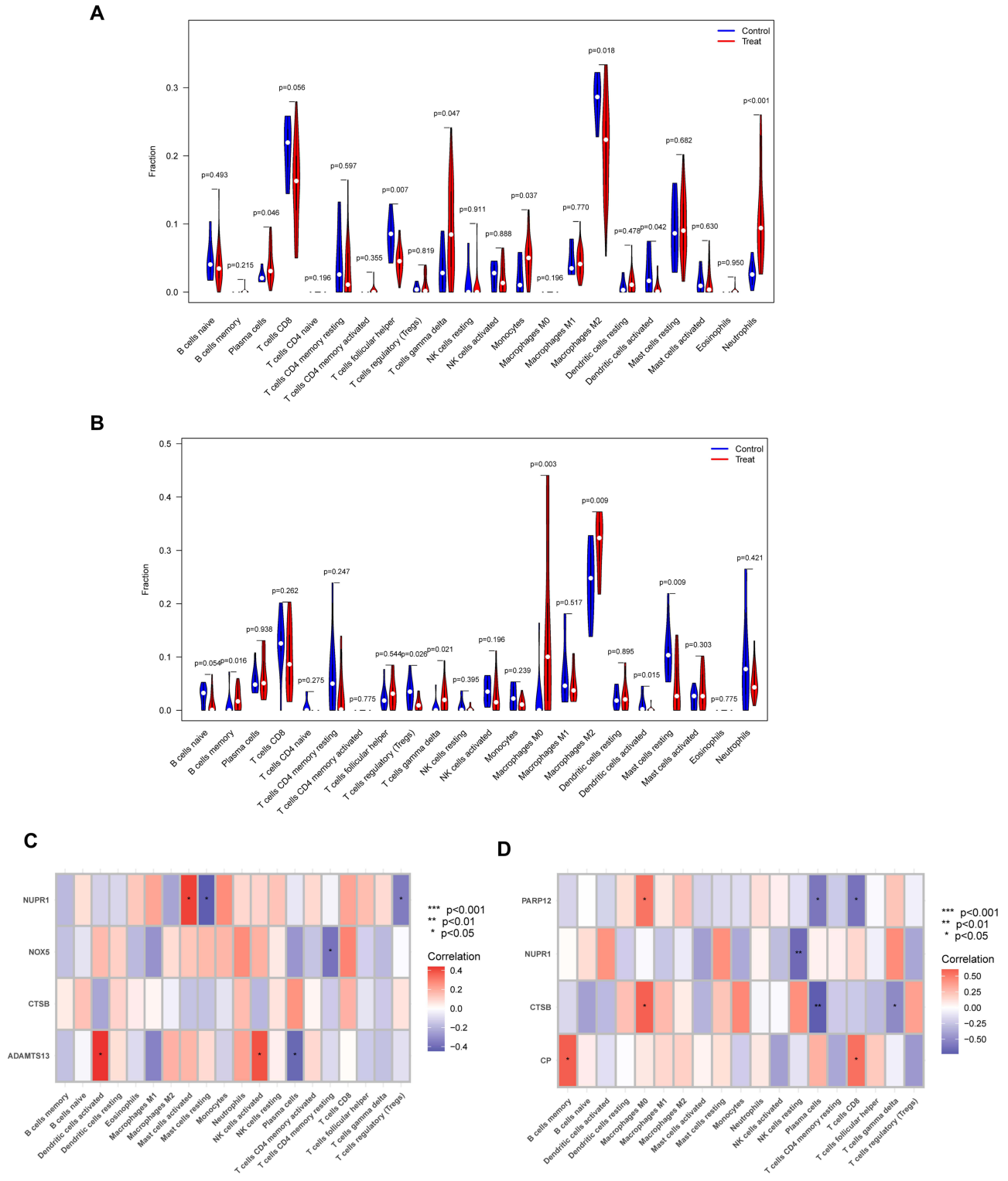

Figure 10 Analysis of immune cell infiltration landscape in AF, AS patients.(**A** and **B**) Implemented the CIBERSORT algorithm to explore the differences in the immune microenvironment between AF, AS patients and normal samples. (**C** and **D**) Mast cells resting and activated had strong positive and negative correlations with NUPR1 in AF. CTSB was positively correlated with macrophages M0 while NUPR1 was negatively correlated with NK cells resting in AS (*p < 0.05, **p < 0.01).

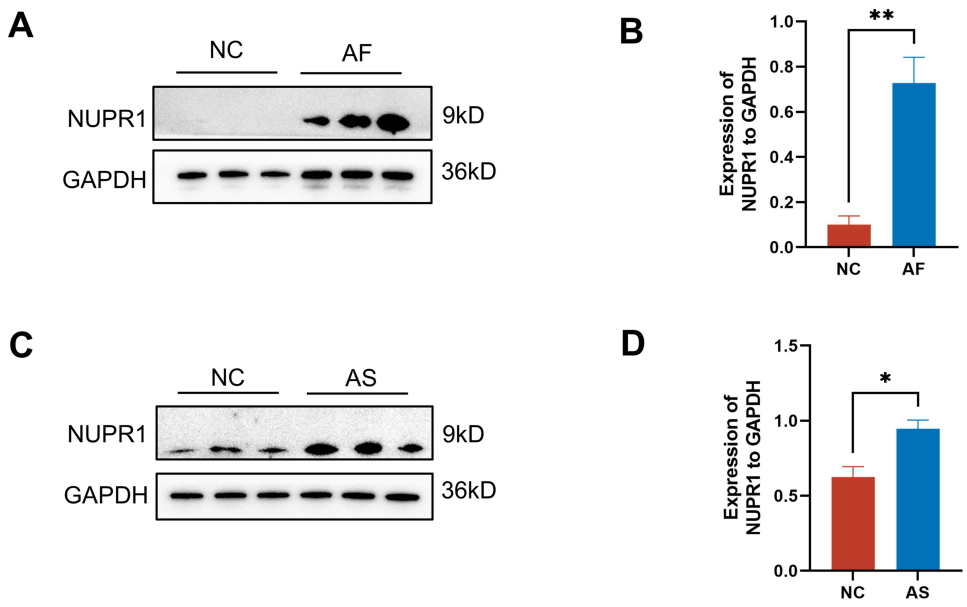

Figure 11 Western blot: (**A-D**) NUPR1 are lowly expressed in normal group and highly expressed in AS. All data were represented as mean ± SEM, n=3. *P <0.05, **P <0.01.

analysis, additional experimental validation of specific DEG mechanisms and transcription factors is needed. Third, the role of identified FDGs in disease progression requires further investigation through in vitro and in vivo studies.

Conclusions

In conclusion, we identified ferroptosis as a potential mechanistic link between AF and AS through the discovery of 47 shared ferroptosis-related genes, particularly NUPR1, and two novel co-diagnostic markers (CSF1R and ITGAM). These findings reveal previously unrecognized molecular connections between the two conditions, extending beyond traditional shared risk factors. While experimental validation is needed, our results suggest new possibilities for developing integrated diagnostic approaches and therapeutic strategies targeting both AF and AS through ferroptosis-related pathways.

Data Sharing Statement

The datasets used in the current work may be found in the databases GEO (https://www.ncbi.nlm.nih.gov/geo/), STRING (https://cn.string-db.org/), GeneMANIA (http://genemania.org/), and TRUST (https://www.grnpedia.org/trrust/). The corresponding author will provide all data and R scripts used in this work upon reasonable request.

Ethics Approval and Consent to Participate

Studies involving human data were reviewed and approved by the Ethics Committee of Yantai Yuhuangding Hospital (Approval NO: 2024-708).

Acknowledgments

The authors would like to thank everyone who took part in the associated conversations.

Author Contributions

All authors made a significant contribution to the work reported, whether that is in the conception, study design, execution, acquisition of data, analysis and interpretation, or in all these areas; took part in drafting, revising or critically reviewing the article; gave final approval of the version to be published; have agreed on the journal to which the article has been submitted; and agree to be accountable for all aspects of the work.

Funding

Natural Science Foundation of Shandong Province (No. ZR2022MH151 and No. ZR2022QH103).

Disclosure

The authors declare no potential conflicts of interest.

References

1. Kornej J, Borschel CS, Benjamin EJ, Schnabel RB. Epidemiology of atrial fibrillation in the 21st century: novel methods and new insights. *Circ Res*. 2020;127(1):4–20. doi:10.1161/CIRCRESAHA.120.316340
2. Schnabel RB, Yin X, Gona P, et al. 50 year trends in atrial fibrillation prevalence, incidence, risk factors, and mortality in the Framingham heart study: a cohort study. *Lancet*. 2015;386(9989):154–162. doi:10.1016/S0140-6736(14)61774-8
3. Zulkifly H, Lip GYH, Lane DA. Epidemiology of atrial fibrillation. *Int J Clin Pract*. 2018;72(3):e13070. doi:10.1111/ijcp.13070
4. Bundy JD, Heckbert SR, Chen LY, Lloyd-Jones DM, Greenland P. Evaluation of risk prediction models of atrial fibrillation (from the multi-ethnic study of atherosclerosis [Mesa]). *Am J Cardiol*. 2020;125(1):55–62. doi:10.1016/j.amjcard.2019.09.032
5. Pistoia F, Sacco S, Tiseo C, Degan D, Ornello R, Carolei A. The epidemiology of atrial fibrillation and stroke. *Cardiol Clin*. 2016;34(2):255–268. doi:10.1016/j.ccl.2015.12.002
6. Heeringa J, van der Kuip DA, Hofman A, et al. Prevalence, incidence and lifetime risk of atrial fibrillation: the Rotterdam study. *Eur Heart J*. 2006;27(8):949–953. doi:10.1093/eurheartj/ehi825
7. Hansson GK, Hermansson A. The immune system in atherosclerosis. *Nat Immunol*. 2011;12(3):204–212. doi:10.1038/ni.2001
8. Libby P, Buring JE, Badimon L, et al. Atherosclerosis. *Nat Rev Dis Primers*. 2019;5(1):56. doi:10.1038/s41572-019-0106-z
9. Weber C, Noels H. Atherosclerosis: current pathogenesis and therapeutic options. *Nat Med*. 2011;17(11):1410–1422. doi:10.1038/nm.2538
10. Jover E, Marin F, Roldan V, Montoro-Garcia S, Valdes M, Lip GY. Atherosclerosis and thromboembolic risk in atrial fibrillation: focus on peripheral vascular disease. *Ann Med*. 2013;45(3):274–290. doi:10.3109/07853890.2012.732702
11. O'Neal WT, Efird JT, Nazarian S, Alonso A, Heckbert SR, Soliman EZ. Peripheral arterial disease and risk of atrial fibrillation and stroke: the multi-ethnic study of atherosclerosis. *J Am Heart Assoc*. 2014;3(6):e001270. doi:10.1161/JAHA.114.001270
12. Ding WY, Gupta D, Lip GYH. Atrial fibrillation and the prothrombotic state: revisiting Virchow's triad in 2020. *Heart*. 2020;106(19):1463–1468. doi:10.1136/heartjnl-2020-316977
13. Herrington W, Lacey B, Sherliker P, Armitage J, Lewington S. Epidemiology of atherosclerosis and the potential to reduce the global burden of atherothrombotic disease. *Circ Res*. 2016;118(4):535–546. doi:10.1161/CIRCRESAHA.115.307611
14. Libby P. Inflammation in atherosclerosis. *Arterioscler Thromb Vasc Biol*. 2012;32(9):2045–2051. doi:10.1161/ATVBAHA.108.179705
15. Xie Y, Hou W, Song X, et al. Ferroptosis: process and function. *Cell Death Differ*. 2016;23(3):369–379. doi:10.1038/cdd.2015.158
16. Angeli JPF, Shah R, Pratt DA, Conrad M. Ferroptosis inhibition: mechanisms and opportunities. *Trends Pharmacol Sci*. 2017;38(5):489–498. doi:10.1016/j.tips.2017.02.005
17. Dixon SJ, Lemberg KM, Lamprecht MR, et al. Ferroptosis: an iron-dependent form of nonapoptotic cell death. *Cell*. 2012;149(5):1060–1072. doi:10.1016/j.cell.2012.03.042
18. da Silva RM. Influence of inflammation and atherosclerosis in atrial fibrillation. *Curr Atheroscler Rep*. 2017;19(1):2. doi:10.1007/s11883-017-0639-0
19. Yang Z, Shen W, Rottman JN, Wikswo JP, Murray KT. Rapid stimulation causes electrical remodeling in cultured atrial myocytes. *J Mol Cell Cardiol*. 2005;38(2):299–308. doi:10.1016/j.yjmcc.2004.11.015
20. Brundel BJ, Shiroshita-Takeshita A, Qi X, et al. Induction of heat shock response protects the heart against atrial fibrillation. *Circ Res*. 2006;99(12):1394–1402. doi:10.1161/01.RES.0000252323.83137.fe
21. Xu B, Li H, Chen H, et al. Identification and prediction of molecular subtypes of atherosclerosis based on m6A immune cell infiltration. *Biochim Biophys Acta Gen Subj*. 2023;1868(2):130537. doi:10.1016/j.bbagen.2023.130537
22. Zheng PF, Zhou SY, Zhong CQ, et al. Identification of m6A regulator-mediated RNA methylation modification patterns and key immune-related genes involved in atrial fibrillation. *Aging*. 2023;15(5):1371–1393. doi:10.18632/aging.204537
23. Haghikia A, Zimmermann F, Schumann P, et al. Propionate attenuates atherosclerosis by immune-dependent regulation of intestinal cholesterol metabolism. *Eur Heart J*. 2022;43(6):518–533. doi:10.1093/eurheartj/ehab644
24. Koelwyn GJ, Corr EM, Erbay E, Moore KJ. Regulation of macrophage immunometabolism in atherosclerosis. *Nat Immunol*. 2018;19(6):526–537. doi:10.1038/s41590-018-0113-3
25. Wei B, Huang X, Lu Y, Xie D, Wei G, Wen W. Screening of atrial fibrillation diagnostic markers based on a GEO database chip and bioinformatics analysis. *J Thorac Dis*. 2022;14(12):4773–4784. doi:10.21037/jtd-22-1457
26. Wu K, Chen H, Li F, Meng X, Chen L, Li N. Identification of potential biomarkers for atrial fibrillation and stable coronary artery disease based on WGCNA and machine algorithms. *BMC Cardiovasc Disord*. 2024;24(1):401. doi:10.1186/s12872-024-04062-z
27. Sun J, Qiao Y, Zhao M, Magnussen CG, Xi B. Global, regional, and national burden of cardiovascular diseases in youths and young adults aged 15-39 years in 204 countries/territories, 1990-2019: a systematic analysis of global burden of disease study 2019. *BMC Med*. 2023;21(1):222. doi:10.1186/s12916-023-02925-4
28. Sarraju A, Nissen SE. Atherosclerotic plaque stabilization and regression: a review of clinical evidence. *Nat Rev Cardiol*. 2024;21(7):487–497. doi:10.1038/s41569-023-00979-8
29. Dobrev D, Heijman J, Hiram R, Li N, Nattel S. Inflammatory signalling in atrial cardiomyocytes: a novel unifying principle in atrial fibrillation pathophysiology. *Nat Rev Cardiol*. 2023;20(3):145–167. doi:10.1038/s41569-022-00759-w
30. Hijazi Z, Oldgren J, Siegbahn A, Granger CB, Wallentin L. Biomarkers in atrial fibrillation: a clinical review. *Eur Heart J*. 2013;34(20):1475–1480. doi:10.1093/eurheartj/eht024
31. Troughton RW, Crozier I. Fine tuning risk stratification for atrial fibrillation. *J Am Coll Cardiol*. 2013;61(22):2285–2287. doi:10.1016/j.jacc.2013.02.066

32. Shibasaki I, Otani N, Ouchi M, et al. Utility of growth differentiation factor-15 as a predictor of cardiovascular surgery outcomes: current research and future directions. *J Cardiol*. 2024;83(3):211–218. doi:10.1016/j.jjcc.2023.08.013
33. Quesada A, Lopez-Valero L, Marcaida-Benito G, et al. Prognostic value of troponin I in atrial fibrillation. *Prog Cardiovasc Dis*. 2021;67:80–88. doi:10.1016/j.pcad.2021.02.012